Radiat Environ Biophys (2001) 40:69–76

ORIGINAL PAPER

Kimiaki Saito · Alfred Wittmann · Sukehiko Koga
Yoshihiro Ida · Tetsuya Kamei · Jun Funabiki
Maria Zankl

Construction of a computed tomographic phantom for a Japanese male adult and dose calculation system

Received: 25 January 2000 / Accepted: 23 October 2000

Abstract Computational human phantoms have been widely used to estimate organ doses and other dosimetric quantities related to the human body where direct measurements are difficult to perform. In recent years, voxel phantoms (voxel = volume element) based on computed tomographic (CT) data of real persons have been constructed which provide a realistic description of the human anatomy. A CT phantom of a Japanese male adult with an average body size was developed as the first Asian voxel phantom. The segmented phantom consists of more than 100 regions enabling the calculation of doses for various parts of the body. The bone marrow distribution was precisely modelled according to the CT values. The EGS4 Monte Carlo transport code was combined with the phantom to calculate organ doses for external exposure due to photons and electrons up to 1 TeV. The calculated organ doses were compared with respective data using MIRD-type mathematical phantoms. In some cases, significant discrepancies in doses were observed, demonstrating the necessity of sophisticated models for accurate dose calculations.

K. Saito (✉)
Japan Atomic Energy Research Institute,
Department of Health Physics, Tokai-mura, Ibaraki-ken,
319-1195 Japan
e-mail: komei@popsvr.tokai.jaeri.go.jp
Tel.: +81-292-826167, Fax: +81-292-826768

A. Wittmann · M. Zankl
GSF–National Research Center for Environment and Health,
Institute of Radiation Protection, 85764 Neuherberg, Germany

S. Koga · Y. Ida · T. Kamei
Fujita Health University Hospital, Department of Radiology,
1-98 Dengakugakubo, Kutsukake-cho, Toyoake, Aichi-ken,
470-1192 Japan

J. Funabiki
Mitsubishi Research Institute, Research Center for Safety Science,
Otemachi, Chiyoda-ku, Tokyo, 100-0004 Japan

Introduction

To properly estimate the risk due to radiation exposure, the organ and tissue doses (hereafter referred to as organ doses) must be accurately determined. Since organ doses cannot be measured directly, it is necessary to use human models, so-called phantoms, to evaluate them. Monte Carlo simulations using computational phantoms are a powerful tool and have therefore been widely used.

The history of computational human phantoms started with mathematical phantoms that defined the shapes of a body as well as organs and tissues by combinations of mathematical equations [1, 2]. These types of phantoms have been widely used for radiation protection, diagnosis and therapy purposes [3, 4, 5, 6, 7, 8, 9, 10]. The body and organ shapes as well as the positional relationships among the organs of these phantoms are somewhat different from real human characteristics, since mathematical expressions do not describe the human body structures in detail.

As an improvement, a new type of phantom has been introduced which is constructed from computed tomographic (CT) data of real persons [11, 12, 13, 14, 15]. In these tomographic phantoms, organs and tissues are defined by sets of small cuboid units called voxels; thus, any shape can be reconstructed with a resolution corresponding to the voxel size.

Based on image data from Caucasian persons, several CT phantoms have been constructed and compared with the mathematical phantoms with regard to their structural characteristics and calculated doses [16, 17, 18, 19]. Certain differences in dose have been observed and particularly for internal exposure, the specific absorbed fractions of energy (SAF) indicated large differences in many cases [18, 19].

The purpose of this study was to construct a CT phantom of a Japanese male adult and to employ it for organ dose calculations. There have previously been some trials to calculate organ doses for Japanese population groups and primarily for the dose assessment of the Hiroshima and Nagasaki survivors, several Japanese phan-

toms at different ages have been used [20]. Furthermore, an attempt has been made to express organ doses as functions of body weight for environmental γ-rays, and to derive organ doses for the Japanese population from those calculated for Caucasians using these functions with the respective body weight [21]. However, no attempt has been made so far to construct CT phantoms for Asian people.

In this paper, the construction procedure, the characteristics of the resulting phantom, and the combination of a radiation transport code system with the phantom is described. Furthermore, some examples of calculated external doses using the phantom will be presented to demonstrate the importance of using realistic phantoms for dose calculations.

Materials and methods

Construction of the CT phantom

Computed tomographic images of a Japanese male adult were taken using a Toshiba Xvigor Laudator at Fujita Health University Hospital. Each slice of the CT images included 512×512 pixels (pixel = picture element) with dimensions of 0.98×0.98 mm^2 and a slice thickness of 1 cm.

For segmentation, i.e. the procedure which assigns each pixel of a CT picture to a specific organ or tissue according to its "grey value" and location, the commercially available image processing equipment MIPRON [22] comprising hardware as well as software was used. Later, some minor modifications of the constructed phantom were made using another commercial software called Visilog 4 [23] on an SGI (Silicon Graphics Inc.) workstation. Although the basic techniques for segmentation compiled in the previous development of the voxel phantoms at GSF – National Research Center for Environment and Health [12, 13, 15] were employed, for many organs and tissues the procedures had to be adjusted to the present CT data set.

The main flow of the segmentation is as follows: irrelevant structures, such as the patients bed, cylindrical container, etc. were removed before starting the segmentation. As a first approximation, the pixels belonging to specific organs and tissues were selected by extracting binary images from the original data using specific ranges of grey values. This procedure is not sufficient for determining the correct shapes of organs and tissues except some special cases having high contrast of grey values to the surrounding tissues, such as air cavities, bones, and lungs. In most cases, further processing of the extracted binary images was necessary. This was done mainly by utilising standard morphological operations, such as dilation, erosion, filling, opening and closing; often plural binary images extracted using different sets of threshold grey values were combined to obtain appropriate shapes. The skin was assumed to be one voxel layer at the outer surface of the body, which resulted in a skin thickness of 0.98 mm, corresponding reasonably closely with the 1.3 mm quoted for the thickness of epidermis and dermis of the Reference man [24]. The segmentation was performed from the top of the CT data (head part) downward slice by slice.

All voxels belonging to the same organ or tissue were given the same organ-specific identification number. Consequently, the set of all voxels having the same identification number makes an organ or tissue, and the combination of these organs and tissues makes a phantom. In this study, more than 100 separate objects were defined and assigned different identification numbers. For example, each rib was given a different number; thus, the dose for each bone piece can be calculated, although this is generally not relevant for prevalent radiation protection considerations.

The density and elemental compositions of an organ or tissue are assumed to be constant over the organ or tissue except for bone. The densities of bone voxels vary greatly, because the proportions of tissues composing bones vary greatly throughout the skeleton. In this study the bone was assumed to consist of two different tissues (i.e. compact bone and bone marrow) and the weight fractions of these tissues in each voxel were determined by interpolation from the original grey values [12, 13, 15]. This method does not allow to distinguish active from inactive marrow, therefore, we used some additional information on the distribution of active marrow in the adult skeleton [25]. According to Cristy [25], the entire marrow located in the lower leg bones and lower arm bones was assumed to be inactive. In all other bone sites, both active and inactive marrow are assumed to be present, and for dosimetric purposes there is no necessity to distinguish these tissues.

In mathematical phantoms, bone is generally assumed to be a homogeneous mixture of compact bone and bone marrow. To obtain bone marrow dose, corrections have been used for considering the relative amount of red bone marrow in a bone, the difference in attenuation properties between the mixture and bone marrow, and a dose enhancement to the red bone marrow due to secondary electrons produced in hard bone [26]. In the voxel phantom, the proportions of bone marrow and hard bone in each voxel can be treated separately by the radiation transport code; thus, we avoided the use of correction factors.

The three-dimensional array describing the segmented phantom Otoko by organ identification numbers, voxel by voxel, requires 90 MB storage on a computer. However, the compressed format devised at GSF specifically for organ dose calculations [13, 15] reduces the space required to 6 MB.

Physical characteristics of the segmented phantom

Table 1 shows the outer dimensions and total mass of the segmented phantom, which has the same height as the standard Japanese male defined by Tanaka et al [27]. The body mass of 65 kg is greater than that of the standard Japanese male, which is 60 kg.

Table 2 compares the masses of organs and tissues of the segmented phantom and the standard Japanese male. Except for small organs with masses below 50 g, the masses of more than half of the tabulated main organs agree with those for the standard Japanese male within 20%, and the masses of most organs within 50%. A large discrepancy is observed for the spleen whose size is only about half that of the standard Japanese man. This is surprising, because the spleen is an organ with a good grey-value contrast to the surroundings and is easily identified on the CT slice images. Furthermore, it is a large organ, and thus the voxel resolution does not have any major consequence, which indicates a significant individual deviation of Otoko's spleen size from that of the standard Japanese male.

Generally, the discrepancy from the average tends to be larger for small organs. This may be partly attributed to the so-called "partial volume effect", i.e. surface voxels, which in reality contain proportions belonging to the organ and proportions belonging to some other structure, have to be assigned one single identification number. This means that they are entirely included in or excluded from the organ under consideration, and this biases the shape and mass of the organ. The magnitude of this effect depends on the spatial resolution of the scan data and the surface-to-volume ratio of an organ.

Table 1 Physical characteristics of the voxel phantom

Parameter	Size
Weight	65 kg
Height	170 cm
Width	48 cm
Depth	23 cm
Slice thickness	10 mm
Pixel side length	0.98 mm

Table 2 Comparison of organ and tissue masses of the voxel phantom and the standard Japanese male

Organ or tissue	Weight (g)		Ratio
	Otoko	Standard Japanese male	
Adrenals	20.9	14	1.49
Eyes	20.0	15	1.33
Lenses	0.2	0.4	0.50
Gall bladder	4.8	8	0.60
Oesophagus	16.1	40	0.40
Stomach	122	140	0.87
Intestine	1009	920	1.10
Small intestine	691	590	1.17
Large intestine	318	330	0.96
Upper large intestine	175	180	0.97
Lower large intestine	143	150	0.95
Heart	476	360	1.32
Kidney	266	320	0.83
Liver	1191	1600	0.74
Lungs	1546	1100	1.41
Pancreas	109	130	0.84
Skeleton	11368	8300	1.37
Hard bone	7582	4500	1.68
Bone marrow	3786	3800	1.00
Skin	2195	2400	0.91
Spleen	75.7	140	0.54
Testes	27.4	37	0.74
Thymus	4.58	33	0.14
Thyroid	9.93	19	0.52
Trachea	8.93	9	0.99
Urinary bladder	38.8	40	0.97

The effect of voxel size on calculated dose for external photon exposure was examined using a voxel version of a MIRD-type phantom by Jones [16], and it was concluded that a voxel size of 2×2×2 mm^3 gives a sufficiently accurate approximation for organ dose calculations as well as organ masses. Furthermore, in his study, the difference in calculated dose between original and voxel-type MIRD phantoms was found to be generally smaller than the difference in organ mass originating from the voxelisation. In our current work, we use voxels of 0.98×0.98×10 mm^3. Despite the volume of this voxel (9.5 mm^3) being not much different from the volume of 2 mm cubic voxel (8 mm^3), the shape is biased in the z-direction.

In order to examine the effect of the biased shape of the voxel on the organ mass representation, the adult male mathematical model (Adam) [4] was voxelised using the same voxel shape, and the resulting organ masses were compared with the original masses. Adam was divided into voxels with dimensions of 0.98×0.98×10 mm^3, and the number of voxels belonging to each organ or tissue was counted. A voxel was considered to belong to a certain organ or tissue when its centre was within the organ or tissue. In addition, the coordinates of the voxel lattice were gradually shifted, and the influence of the exact lattice position on the masses of the voxelised organs and tissues was investigated.

In most cases, the mass of the voxelised organ agreed with the original mass within 10%, and for large organs the differences did not exceed a few percent. The maximum difference observed was 20%. This indicates that small deviations in organ mass between Otoko and the standard Japanese male could partly be explained by the voxelisation and the resulting partial-volume effect, but large deviations are due to individual variations of organ size.

Two-dimensional images of the voxel phantom were obtained by using MIPRON and Visilog 4 and also a commercial image processing code AVS [28] was modified to produce three-dimensional views of the voxel phantom. Examples of internal two-dimensional and three-dimensional views of the phantom are shown in Fig. 1.

Fig. 1 Anterior three-dimensional view and cross section at shoulder level of the developed phantom

Development of the dose calculation system

A system for the calculation of organ doses for external exposure of photons and electrons (UCPIXEL) was developed on the basis of the EGS4 Monte Carlo code [29]. EGS4 can consider photon-electron cascade processes precisely and it can simulate the transport of photons and electrons up to 1 TeV. As photon interaction processes, photoelectric absorption, coherent scattering, Compton scattering and pair production are considered. An electron or a positron is assumed to deposit the energy continuously and the scattered direction is determined by Moliere's multiple-scattering theory. Energy loss by Bremsstrahlung and δ-ray emissions is considered as well.

The following five different types of elemental tissue compositions in a human body are considered in the transport calculation: soft tissue, lung tissue, skin, bone, and bone marrow. Furthermore, air and soil can be simulated in the transport calculation. The effect of elemental compositions on external doses was investigated by Jones using the voxel phantom NORMAN [17] and it was found that five or six sets of material are sufficient to represent the elemental composition of a human body.

Idealised exposure conditions are simulated using parallel uniform photon or electron beams irradiating from the following geometries: antero-posterior (AP), postero-anterior (PA), left lateral (LLAT), right lateral (RLAT), from above (AB), from below (BA), rotational (ROT), and isotropic (ISO).

To simulate an exposure in the environment, the system can consider the incidence of photons having non-uniform energy and angular distributions. This is achieved by using a hypothetical cy-

lindrical source around the phantom which emits photons according to a distribution function of energy and angle obtained from a photon transport calculation in the environment carried out separately. The validity of this procedure has been proved [30].

Furthermore, a uniform volume source around the phantom and a uniform plane source in the ground which emit photons or electrons can be simulated. In these simulations, the existence of the air and soil around the phantom was considered on the assumption that the phantom stands up-right on the ground. The consideration of scattering of electrons by the air and soil is expected to be important when realistic external exposure is simulated, because the radiation field can be easily perturbed by the existence of air and soil. In the case of the hypothetical cylindrical source for environmental γ-rays described above, the effect of air and soil is already included in the probability density functions used to sample the initial photon conditions.

Results and discussion

Organ doses for photons

Examples of the calculated results for photons are shown in Table 3 and Fig. 2. The calculated organ doses were compared with doses for Adam, a sex-specific MIRD-type phantom [4] and Golem, a CT phantom [15], both of which were developed at GSF. Both phantoms model Caucasian male adults, and the same photon transport calculation code is used for dose calculation.

The differences in doses among these phantoms are affected by:

a. The difference in body size between Caucasians and Japanese
b. The difference in modelling the human body (mathematical or voxel-based) and the resulting difference in structures such as shapes and positions of organs
c. Deviations in the individual anatomy compared to that of a standard person
d. The difference in transport calculation methods.

In Table 3, organ doses for AP-geometry photons and four different energies were compared for Otoko and Adam. Generally, the difference in doses for photons between Adam and Otoko is not large, however, for some organs or tissues the doses indicate significant deviations between the phantoms. There is a tendency of the deviations to be large at low energies where the attenuation of photons is large and the organ doses are sensitive to the detailed internal geometry of the phantoms.

The maximum deviations in dose are two- to threefold at 40 keV and occur for stomach, bladder, esophagus, adrenals and kidneys. These organs are located deep in the human body and the attenuation of photons is affected by the position. The position differences are considered to be the major reason of dose discrepancies for these organs. In general, the discrepancies decrease with increasing energy. For higher energies, i.e. above 1 MeV, the dose discrepancies for these organs are not significant.

Figure 2 shows the energy dependence of organ doses for Otoko, Adam and Golem. The dose calculations for Adam and Golem were performed with the photon transport calculation code used at GSF. The electrons were assumed to deposit their energies at the locations where they are generated: the so-called kerma approximation was used which is valid when a secondary particle equilibrium exists, and it has been proved to be acceptable in many cases.

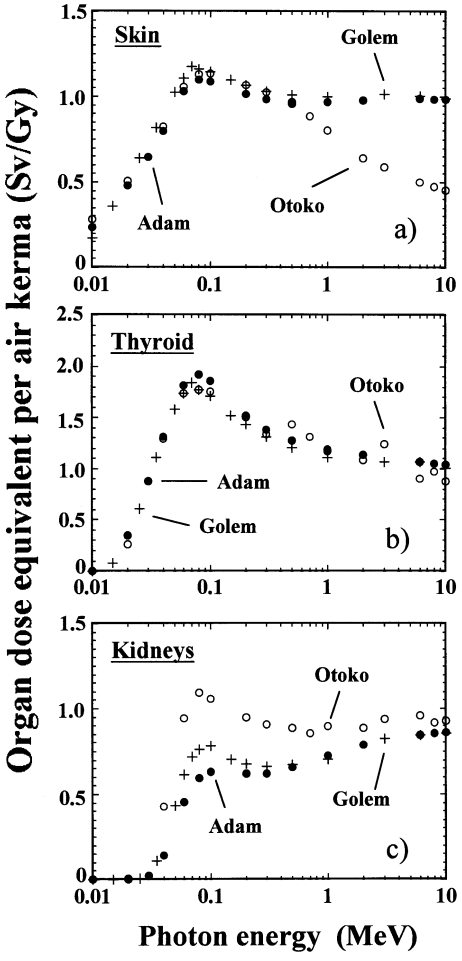

Fig. 2 Comparison of organ doses among the developed voxel phantom Otoko, a Caucasian voxel phantom Golem, and a MIRD-type male phantom Adam for some selected organs

In the dose calculations for Otoko using EGS4, the transport of secondary electrons was simulated. At the interface between the body and the outer space, the condition of a secondary particle equilibrium is violated, since the secondary electrons which are produced in the air and enter the body are not considered in this calculation. With increasing energy, the electron ranges become large enough that the energy of secondary electrons is carried into the inner part of the body or escapes from the body, in comparison with the kerma approximation. There is a maximum effect at the body surface.

The skin dose for Otoko at 10 MeV is lower than for Adam and Golem by a factor of 2. In the energy region below 500 keV, the electron transport does not have a significant effect, and the skin doses for the three phantoms are similar. This shows that the skin dose is not sensitive to the individual phantom geometry. Concern-

Table 3 Comparison of organ doses between the voxel phantom and a MIRD-type phantom for monoenergetic parallel photons incident from AP geometry

Organ	Organ dose equivalent per air kerma (Sv/Gy)											
	40 keV			100 keV			1 Mev			10 MeV		
	Otoko	Adam	Ratio	Otoko	Adam	Ratio	Otoko	Adam	Ratio	Otoko	Adam	Ratio
Bone marrow	3.25E–01	2.05E–01	1.59	1.02E+00	8.06E–01	1.27	1.00E+00	7.83E–01	1.28	1.05E+00	9.22E–01	1.14
Colon	8.06E–01	6.34E–01	1.27	1.46E+00	1.40E+00	1.04	1.00E+00	1.01E+00	0.99	9.33E–01	9.82E–01	0.95
Lungs	7.81E–01	7.62E–01	1.02	1.33E+00	1.36E+00	0.98	1.04E+00	1.03E+00	1.01	9.92E–01	9.89E–01	1.00
Stomach	5.45E–01	9.80E–01	0.56	1.28E+00	1.66E+00	0.77	9.42E–01	1.07E+00	0.88	9.58E–01	9.75E–01	0.98
Bladder	5.11E–01	9.64E–01	0.53	1.22E+00	1.67E+00	0.73	1.08E+00	1.07E+00	1.01	1.06E+00	9.48E–01	1.12
Liver	8.00E–01	7.13E–01	1.12	1.42E+00	1.40E+00	1.02	9.98E–01	9.99E–01	1.00	9.42E–01	9.90E–01	0.95
Oesophagus	5.02E–01	2.57E–01	1.95	1.22E+00	9.12E–01	1.34	9.17E–01	8.22E–01	1.12	1.00E+00	9.62E–01	1.04
Thyroid	1.29E+00	1.31E+00	0.98	1.75E+00	1.86E+00	0.94	1.17E+00	1.19E+00	0.98	8.61E–01	1.05E+00	0.82
Skin	8.22E–01	7.98E–01	1.03	1.14E+00	1.09E+00	1.04	8.04E–01	9.70E–01	0.83	4.52E–01	9.83E–01	0.46
Hard bone	2.10E+00	1.25E+00	1.69	2.48E+00	1.78E+00	1.39	8.69E–01	8.82E–01	0.99	8.05E–01	9.67E–01	0.83
Adrenals	2.97E–01	1.61E–01	1.84	7.99E–01	7.02E–01	1.14	7.63E–01	7.09E–01	1.08	9.17E–01	8.84E–01	1.04
Brain	2.23E–01	2.80E–01	0.80	8.10E–01	8.17E–01	0.99	8.43E–01	8.29E–01	0.92	9.37E–01	9.30E–01	1.01
Small intestine	9.50E–01	5.74E–01	1.66	1.63E+00	1.36E+00	1.20	1.08E+00	9.68E–01	0.87	9.50E–01	9.40E–01	1.01
Kidney	4.26E–01	1.43E–01	2.98	1.06E+00	6.30E–01	1.68	8.96E–01	7.24E–01	1.24	9.29E–01	8.62E–01	1.08
Muscle	5.93E–01	6.65E–01	0.89	1.08E+00	1.16E+00	0.93	9.49E–01	9.46E–01	1.00	8.59E–01	9.64E–01	0.89
Pancreas	6.54E–01	4.38E–01	1.49	1.37E+00	1.25E+00	1.09	9.93E–01	9.27E–01	1.07	9.50E–01	9.55E–01	0.99
Spleen	3.18E–01	2.96E–01	1.07	9.35E–01	9.27E–01	1.01	7.90E–01	8.37E–01	0.94	9.57E–01	9.19E–01	1.04
Thymus	8.45E–01	1.21E+00	0.70	1.67E+00	1.89E+00	0.88	1.05E+00	1.10E+00	0.95	9.59E–01	8.56E–01	1.12
Testes	1.42E+00	1.51E+00	0.94	1.89E+00	1.86E+00	1.02	1.15E+00	1.18E+00	0.98	5.55E–01	1.00E+00	0.55
Average	7.10E–01	6.47E–01	1.10	1.32E+00	1.26E+00	1.04	9.55E–01	9.37E–01	1.02	9.18E–01	9.49E–01	0.97

ing the radiation transport calculation method, it can be concluded that for skin the kerma approximation is not valid for photon energies above approximately 500 keV. In reality, electrons produced in air around the body enter the body and partly compensate this dose reduction, but the effect is assumed to be small.

The doses for the thyroid show good agreement among the three phantoms in the whole energy region considered. This indicates that the thyroid glands are located at similar depths for the three phantoms for AP irradiation geometry and furthermore they are deep enough to realise the secondary electron equilibrium.

The discrepancy in kidney doses is considered to result from the difference in organ positions and body size. In Otoko and Golem, the kidneys are located almost centrally in the trunk, while in Adam they are much closer to the rear trunk side. This results in larger kidney doses for both voxel phantoms compared to Adam. In addition, the body weight of Otoko is reduced by 5 kg compared to that of Adam or Golem, therefore the the kidneys of Otoko are shielded by a thinner layer of overlaying tissues, which leads to a further increase in Otoko's kidney dose. These factors contribute to the dose difference between Otoko and Adam.

There are significant dose differences among the phantoms for several organs even with regard to photon exposure. Therefore, body phantoms with a more realistic anatomy, such as the voxel models, are desirable for a variety of situations in order to derive reliable dose values for the population considered.

Organ doses for electrons

Two different energies of 5 MeV and 100 MeV were considered for electron incidence. Our results are compared with the data of Ferrari et al. [9] using a MIRD-type hermaphrodite phantom in Table 4. In the case of 100 MeV, the doses for all organs and tissues are similar for the Japanese voxel phantom and the MIRD phantom, because the electrons at this energy deposit energy homogeneously in the human body due to their long range (about 30 cm) and the exact organ positions are therefore of minor relevance.

On the other hand, in the case of 5 MeV electrons where the range in tissue is about 2.5 cm, the organ doses are significantly different between the Japanese voxel phantom and the MIRD phantom. Here the depth of the organ in the body is of great consequence. For tissues distributed widely over the whole body, such as muscles, there is generally no major variety, since local dose differences are compensated by averaging the dose over the body. However, the dose differences for single organs are significant.

The tendency of the differences cannot simply be explained by the size of the phantoms. For example, most organ doses of the Japanese phantom exceed those of the MIRD phantom, as may be expected due to the reduced shielding effect of the smaller body size. In contrast, the

Table 4 Comparison of organ doses between the voxel phantom and a MIRD-type phantom for monoenergetic electrons incident from AP geometry

Organ	Organ dose equivalent per electron fluence (Sv cm^2)					
	5 MeV			100 MeV		
	Otoko	MIRD	Ratio	Otoko	MIRD	Ratio
Bone marrow	2.82E–11	1.84E–11	1.53	3.72E–10	3.62E–10	1.03
Colon	1.39E–11	5.39E–13	25.8	3.42E–10	3.50E–10	0.98
Lung	4.57E–12	4.31E–13	10.6	3.69E–10	3.75E–10	0.98
Stomach	5.28E–13	3.27E–11	0.02	3.62E–10	3.53E–10	1.03
Bladder	4.67E–11	5.82E–12	8.02	3.71E–10	3.36E–10	1.10
Liver	6.19E–12	2.88E–12	2.15	3.49E–10	3.47E–10	1.01
Oesophagus	8.48E–12	3.26E–13	26.0	3.55E–10	3.91E–10	0.91
Thyroid	8.75E–11	1.26E–10	0.69	3.37E–10	3.40E–10	0.99
Skin	1.82E–10	2.91E–10	0.63	3.20E–10	3.22E–10	0.99
Bone surface	3.74E–11	8.61E–12	4.34	3.17E–10	3.47E–10	0.91
Adrenals	3.48E–13	1.72E–13	2.02	3.63E–10	3.39E–10	1.07
Brain	2.47E–12	3.12E–12	0.79	3.59E–10	3.53E–10	1.02
Small intestine	3.35E–12	4.38E–13	7.65	3.48E–10	3.57E–10	0.97
Kidney	3.05E–13	2.89E–13	1.06	3.64E–10	3.70E–10	0.98
Muscle	5.39E–11	4.98E–11	1.08	3.49E–10	3.47E–10	1.01
Pancreas	5.57E–13	3.94E–13	1.41	3.60E–10	3.74E–10	0.96
Spleen	3.04E–13	4.38E–13	0.69	3.54E–10	3.68E–10	0.96
Thymus	6.46E–11	3.54E–11	1.82	3.21E–10	3.48E–10	0.92
Average	3.01E–11	3.20E–11	0.94	3.51E–10	3.54E–10	0.99

stomach dose for the Japanese phantom is much lower than that for the MIRD phantom; there are also further organs (thyroid, skin, brain) receiving lower doses than those for the MIRD phantom. For some organs such as colon, lungs, stomach and esophagus, the dose differs by more that one order of magnitude. This shows that the exact organ position has an important influence on organ doses for electrons and other charged particles having small ranges compared to the body size.

Conclusions

A voxel-type phantom based on CT data of an Asian person was developed for the first time. The phantom has a body size close to the Japanese standard male defined by Tanaka et al. [27], but some of the organ and tissue masses differ from those of the Japanese standard male. The differences are small for larger main organs, but they are significant for some small organs. Since the voxelisation using voxels of 0.98×0.98×10 mm^3 was found to mis-convert the organ size by about 20% at maximum, the main reason for the significant deviation is considered to be due to individual fluctuation.

The EGS4 transport calculation code which allows external organ doses for a photon-electron cascade up to 1 TeV to be calculated, was combined with the voxel phantom. Calculated organ doses for photons and electrons were compared with data using MIRD-type phantoms and a CT phantom for a Caucasian adult male. In the case of photons, some dose discrepancies due to the difference in phantom anatomy were observed, mainly in the low energy region. For electrons at low energy where the range is small compared to the body size, significant dose differences of nearly two orders of magnitude were observed.

These findings illustrate a realistic description of the body for the calculation of relevant organ dose data, especially in the lower energy ranges of both photons and electrons. According to individual deviations of the present phantom's anatomy from that of the standard Japanese male, the calculated doses may have certain limitations concerning their applicability to a general population. However, in the absence of a realistic model exactly describing the standard Japanese male, the present phantom is considered to be the most suitable for dose calculations relevant to the Japanese population.

Acknowledgements We are grateful to Dr. Nelson of SLAC, Dr. Hirayama of KEK, and the persons concerned for providing us with a copy of the Monte Carlo code EGS4.

References

1. Snyder WS, Fisher HL, Ford MR, Warner GG (1969) Estimates of absorbed fractions for monoenergetic photon sources uniformly distributed in various organs of a heterogeneous phantom. MIRD Pamphlet No. 5. J Nucl Med 10 [Suppl 3]: 7–52
2. Snyder WS, Ford MR, Warner GG (1974) Estimates of absorbed fractions for monoenergetic photon sources uniformly distributed in various organs of a heterogeneous phantom; Revision of MIRD Pamphlet No. 5 ORNL-4979. Oak Ridge National Laboratory, Oak Ridge, Tenn
3. Cristy M (1980) Mathematical phantoms representing children of various ages for use in estimates of internal dose. ORNL/NUREG/TM-367. Oak Ridge National Laboratory, Oak Ridge, Tenn
4. Kramer R, Zankl M, Williams G, Drexler G (1982) The calculation of dose from external photon exposures using reference human phantoms and Monte Carlo methods. Part I: the male (Adam) and female (Eva) adult mathematical phantoms. GSF-Report S-885, National Research Center for Health and Environment, Neuherberg, Germany

5. Yamaguchi Y (1994) Dose conversion coefficients for external photons based on ICRP 1990 Recommendations. J Nucl Sci Technol 31: 716–725
6. Stewart RD, Tanner JE, Leonowich JA (1993) An extended tabulation of effective dose equivalent from neutrons incident on a male anthropomorphic phantom. Health Phys 65: 405–413
7. Kerr GD, Hwang JML, Jones RM (1976) A mathematical model of a phantom developed for use in calculation of radiation dose to the body and major internal organs of a Japanese adult. ORNL/TM-5336. Oak Ridge National Laboratory, Oak Ridge, Tenn
8. Zankl M, Petoussi N, Drexler G (1992) Effective dose and effective dose equivalent-The impact of the new ICRP definition for external photon irradiation. Health Phys 62: 395–399
9. Ferrari A, Pelliccioni M, Pillon M (1997) Fluence to effective dose and effective dose equivalent conversion coefficients for electrons from 5 MeV to 10 GeV. Radiat Prot Dosim 69: 97–104
10. Kai M (1985) Estimation of embryonic and fetal doses from accidentally released radioactive plumes. Radiat Prot Dosim 2: 91–94
11. Dimbylow PJ (1995) The development of realistic voxel phantoms for electromagnetic field dosimetry. In: Dimbylow PJ (ed) Voxel phantom development: Proceedings of the International Workshop.NRPB, Chilton, UK, pp 1–7
12. Zankl M, Veit R, Williams G, Schneider K, Fendel H, Petoussi N, Drexler G (1988) The construction of computer tomographic phantoms and their application in radiology and radiation protection. Radiat Environ Biophys 27: 153–164
13. Veit R, Zankl M, Petoussi N, Mannweiler E, Williams G, Drexler G (1989) Tomographic anthropomorphic models. Part I: Construction technique and description of models of an 8-week-old baby and a 7-year-old child. GSF-Report 3/89. GSF–National Research Center for Health and Environment, Neuherberg, Germany
14. Zubal IG, Harrell CR, Smith EO, Rattner Z, Gindi G, Hoffer PB (1994) Computerized three-dimensional segmented human anatomy. Med Phys 21: 299–302
15. Zankl M, Petoussi-Henss N, Wittmann A (1995) The GSF voxel phantoms and their application in radiology and radiation protection. In: Dimbylow PJ (ed) Voxel phantom development. Proceedings of the International Workshop, NRPB, Chilton, UK, pp 98–104
16. Jones DG (1996) The use of voxel phantoms in organ dose calculations. In: Dimbylow PJ (ed) Voxel phantom development. Proceedings of the International Workshop, NRPB, Chilton, UK, pp 90–97
17. Jones DG (1997) A realistic anthropomorphic phantom for calculating organ doses arising from external photon irradiation. Radiat Prot Dosim 72: 21–29
18. Jones DG (1998) A realistic anthropomorphic phantom for calculating specific absorbed fractions of energy deposited from internal gamma emitters. Radiat Prot Dosim 79: 411–414
19. Petoussi-Henss N, Zankl M (1998) Voxel anthropomorphic models as a tool for internal dosimetry. Radiat Prot Dosim 79: 415–418
20. Kaul DC, Egbert SD, Otis MD, Kuhn T, Kerr GD, Eckerman KF, Cristy M, Maruyama T, Ryman JC, Tang JS (1987) Organ dosimetry. In: Roesch WC (ed) US-Japan joint reassessment of atomic bomb radiation dosimetry in Hiroshima and Nagasaki. Radiation Effects Research Foundation, Hiroshima, Japan, pp 306
21. Saito K, Petoussi N, Zankl M, Veit R, Jacob P, Drexler G (1991) Organ doses as a function of body weight for environmental gamma rays. J Nucl Sci Technol 28: 627–641
22. Kontron Elektronik (1992) MIPRON user's manual, Rel. 2.0. Kontron, Eching, Germany
23. Noesis (1992) Visilog 4 user's guide. Noesis, Orsay, France
24. ICRP (1975) Publication 23. Reference man: anatomical, physiological and metabolic characteristics. International Commission on Radiological Protection. Pergamon Press, Oxford
25. Cristy M (1980) Mathematical phantoms representing children of various ages for use in estimates of internal dose. ORNL/NUREG/TM-367. Oak Ridge National Laboratory, Oak Ridge, Tenn
26. Kramer R (1979) Determination of conversion factors between tissue doses and relevant radiation quantities for external X and gamma radiation. GSF-Report S-556. GSF–National Research Center for Health and Environment, Neuherberg, Germany
27. Tanaka G, Nakahara Y, Nakajima Y (1989) Japanese reference man 1988-IV. Studies on the weight and size of internal organs of normal Japanese. Nippon Acta Radiol 49: 344
28. Stardent Computer (1991) AVS users guide. Stardent Computer, Six New England Tech Center, 521 Virginia Road, Concord, Mass
29. Nelson WR, Hirayama H, Rogers DWO (1985) The EGS4 code system. SLAC-265, Stanford Linear Accelerator Center, Stanford, Calif
30. Saito K, Petoussi N, Zankl M, Veit R, Jacob P, Drexler G (1990) Calculation of organ doses from environmental gamma rays using human phantoms and Monte Carlo methods. Part I: Monoenergetic sources and natural radionuclides in the ground. GSF-Report 2/90. GSF–National Research Center for Health and Environment, Neuherberg, Germany
31. Zankl M, Drexler G, Petoussi-Henss N, Saito K (1997) The calculation of dose from external photon exposures using reference human phantoms and Monte Carlo Methods Part VII: Organ doses due to parallel and environmental exposure geometries. GSF-Report 8/97. GSF–National Research Center for Health and Environment, Neuherberg, Germany